Available online at www.sciencedirect.com
ScienceDirect
Tectonophysics 424 (2006) 319–334
TECTONOPHYSICS
www.elsevier.com/locate/tecto

A way to synchronize models with seismic faults for earthquake forecasting: Insights from a simple stochastic model

Álvaro González [a,*], Miguel Vázquez-Prada [b], Javier B. Gómez [a], Amalio F. Pacheco [b]

[a] Departamento de Ciencias de la Tierra, Universidad de Zaragoza, C./ Pedro Cerbuna, 12. 50009 Zaragoza, Spain
[b] Departamento de Física Teórica and BIFI, Universidad de Zaragoza, C./ Pedro Cerbuna, 12. 50009 Zaragoza, Spain

Received 5 August 2005; received in revised form 11 November 2005; accepted 25 March 2006
Available online 23 June 2006

Abstract

Numerical models are starting to be used for determining the future behaviour of seismic faults and fault networks. Their final goal would be to forecast future large earthquakes. In order to use them for this task, it is necessary to synchronize each model with the current status of the actual fault or fault network it simulates (just as, for example, meteorologists synchronize their models with the atmosphere by incorporating current atmospheric data in them). However, lithospheric dynamics is largely unobservable: important parameters cannot (or can rarely) be measured in Nature. Earthquakes, though, provide indirect but measurable clues of the stress and strain status in the lithosphere, which should be helpful for the synchronization of the models.

The rupture area is one of the measurable parameters of earthquakes. Here we explore how it can be used to at least synchronize fault models between themselves and forecast synthetic earthquakes. Our purpose here is to forecast synthetic earthquakes in a simple but stochastic (random) fault model. By imposing the rupture area of the synthetic earthquakes of this model on other models, the latter become partially synchronized with the first one. We use these partially synchronized models to successfully forecast most of the largest earthquakes generated by the first model. This forecasting strategy outperforms others that only take into account the earthquake series. Our results suggest that probably a good way to synchronize more detailed models with real faults is to force them to reproduce the sequence of previous earthquake ruptures on the faults. This hypothesis could be tested in the future with more detailed models and actual seismic data.

Keywords: Earthquake prediction; Fault model; Cellular automata; Synthetic earthquake catalogues; Seismic modelling; Characteristic earthquakes; Data assimilation

1. Introduction: data assimilation in numerical fault models

Numerical models are now frequently used to simulate the seismic behaviour of faults (e.g. Kato and Seno, 2003; Fitzenz and Miller, 2004; Kuroki et al., 2004) and fault networks (e.g. Ward, 2000; Hashimoto, 2001; Robinson and Benites, 2001; Rundle et al., 2001; Soloviev and Ismail-Zadeh, 2003; Robinson, 2004; Rundle et al., 2004, 2006). In these models, fault planes separate lithospheric blocks that are strained at specific rates, and sudden slips (earthquakes) are generated by the faults according to certain friction and/or rupture laws. Although no completely realistic dynamical model presently exists, these simulations are now sufficiently credible to begin to play a substantial role in scientific studies of earthquake

* Corresponding author. Tel.: +34 610329045; fax: +34 976761106.
E-mail addresses: Alvaro.Gonzalez@unizar.es (Á. González), amalio@unizar.es (A.F. Pacheco).

0040-1951/$ - see front matter © 2006 Elsevier B.V. All rights reserved.
doi:10.1016/j.tecto.2006.03.039

probability and hazard (Ward, 2000). The final goals of the numerical modelling of seismicity are not different from, for example, the goals of numerical models of the atmosphere. A good model should be able to:

(1) reproduce the general characteristics of the system,
(2) mimic the state of the system at the present moment, and
(3) forecast the future evolution of the system.

Most numerical models of seismicity have been designed to achieve the first goal, by reproducing general characteristics of earthquakes such as their size–frequency distribution (e.g. Bak and Tang, 1989; Olami et al., 1992; Dahmen et al., 1998; Preston et al., 2000; Vázquez-Prada et al., 2002), or the generation of aftershocks and foreshocks (e.g. Hainzl et al., 1999). When a model is designed this way, it is left to evolve freely according to its rules, and all that is checked is whether the overall results of the model are similar to the observations made in Nature.

The second goal requires data assimilation, that is, the process of absorbing and incorporating observed information into the model. By this process, the model is tuned and synchronized, at least partially, with the real system it tries to simulate. In a meteorological model, data of atmospheric pressure, temperature, humidity, cloud cover, precipitation, etc. measured in a given moment at different locations and heights can be included. With this procedure, the model becomes a reasonably good representation of the atmosphere at that moment. Then it can be used to calculate the probable future atmospheric evolution (i.e. the third goal cited above).

Seismic data assimilation poses greater problems than its meteorological equivalent. This explains (at least partially) the relative delay in developing reliable forecasts of large earthquakes. The inner workings of both the atmosphere (Houghton, 2002) and the lithosphere (Goltz, 1997; Turcotte, 1997; Keilis-Borok, 2002) are complex and chaotic, so they are inherently difficult to forecast. However, while meteorologists can probe the atmosphere every day at different places and heights (and assimilate the obtained data in their models in near real-time), lithospheric variables of paramount importance, such as the stress and strain, can be measured only in certain places, and not at any time: earthquakes have unobservable dynamics (e.g. Rundle et al., 2003). For example, the best current compendium of stress magnitudes and directions in the lithosphere is the World Stress Map (Zoback, 1992; Reinecker et al., 2005), whose entries are point static time-averaged estimates of maximum and minimum principal stresses in space. And the direct measurements of stress on active fault zones at depth are still scarce (e.g. Ikeda et al., 2001; Tsukahara et al., 2001; Yamamoto and Yabe, 2001; Hickman and Zoback, 2004; Boness and Zoback, 2004). The numerical models would need better spatial and temporal information of stress, both more abundant and more systematically collected than that currently available (Rundle et al., 2004). It is thus necessary to seek ways to tune and synchronize the models with more abundant observable data.

A first step of data assimilation in models of earthquake faults is to introduce information regarding the topology (that is, the shape and location) of the active faults and their long-term behaviour. For example, the long-term fault slip rate, and the average recurrence interval of the largest earthquakes in the fault can be estimated from paleoseismological studies and should be included in the models (Grant and Gould, 2004). Examples of this approach are the works of Ward (2000), Robinson (2004) and Rundle et al. (2006). The surface deformation measured via Global Positioning System (GPS) networks and by Synthetic Aperture Radar Interferometry (InSAR) can also constitute input data for the fault models (Rundle et al., 2004). Earthquakes themselves are indeed the most obvious observable events of lithospheric dynamics, and could provide the most detailed data available to assimilate in the models, but how? The earthquake rupture area could be an important clue.

The rupture area and slip distribution in real earthquakes can be very complex (Sieh, 1996; Kanamori and Brodsky, 2004), but can be estimated in a variety of ways. The slip distribution can be calculated by inverting the observed seismic waveforms (Kanamori and Brodsky, 2004) or tsunami waveforms (e.g. Tanioka et al., 2004; Baba and Cummins, 2005), and/or by geodetic modelling of ground displacement (Yabuki and Matsuura, 1992). Some earthquakes produce surface ruptures, which are useful for estimating the rupture area (Stirling et al., 2002). Although most surface ruptures occur in large shocks, with magnitudes larger than about 6, they have been reported for earthquakes with magnitudes down to 2.5 (see the compilation of historic earthquakes with surface rupture by Yeats et al., 1997, pp. 473–485). Also, the rupture area can be estimated from the seismic moment (calculated from the amplitude spectra of seismic waves; Scholz, 2002; Kanamori and Brodsky, 2004), or from the moment magnitude (Wells and Coppersmith, 1994; Stirling et al., 2002; Dowrick and Rhoades, 2004). Frequently the location of early aftershocks is used to determine the rupture area of the

mainshock (Wells and Coppersmith, 1994), although the aftershock zone tends to grow with time (Kisslinger, 1996) and is not necessarily a good indicator of that area (Yagi et al., 1999).

Complex models with realistic fault topology are able to reproduce the rupture area and co-seismic slip of past earthquakes. It is thus possible to force the model to reproduce the rupture of a past earthquake, and let it evolve from that moment onwards to see what could happen in the future. For example, Ward (2000) developed a model including the network of main faults in the San Francisco Bay Area (California). He forced the model to reproduce the San Andreas Fault surface co-seismic slip of the 1906 San Francisco earthquake, and let it evolve freely from that earthquake onwards, in an attempt to simulate the probable sequence of earthquake ruptures during the next 3000 years.

But considering only the data of the largest earthquake in the series is probably not sufficient to properly synchronize the model. Complex and chaotic systems are very sensitive to the initial conditions. The information regarding only one event probably does not sufficiently constrain the initial conditions, and the calculated evolution will probably be a particular case of a large range of possible outcomes. Will this panorama improve by forcing the model to reproduce all the observed earthquake ruptures, including the small ones? Probably yes. To check whether this idea works, at least to forecast synthetic seismicity, is the purpose of this paper. The number of recorded large earthquakes is relatively scarce, especially in individual faults (where the recorded series very rarely includes ten large events). This hampers the ability to characterize statistically the effectiveness of any forecasting method. Synthetic earthquake catalogues, on the other hand, can be as long as desired. This enables to ascertain, with robust statistics, whether a forecasting strategy could be useful, before endeavouring to apply it to real seismicity.

In the following sections, our goal will be to forecast the largest earthquakes generated by the minimalist model, a simple numerical fault model. We will show that when all the earthquake ruptures generated by this model are imposed on other, similar models, these become partially synchronized with the former. We use them to declare alarms that efficiently mark the occurrence of the largest shocks in the first model. The results are much better than those obtained with other strategies that consider only the earthquake series. The model, albeit simple, is stochastic (it involves randomness), so its efficient forecasting is not trivial. We will describe how this stochasticity can be dealt with, by using an approach similar to the so-called ensemble forecasting used in Meteorology (Palmer et al., 2005). The method could be used in other more detailed and realistic models (stochastic or not) to test our general conclusion: that they might be partially synchronized with actual faults by being forced to reproduce the series of observed earthquake ruptures.

In the next section we describe the model and its properties. Then, we outline the general scheme of prediction and the forecasting strategies used as reference to assess the merits of any other predictive method in the model. Finally, the method based on partial synchronization is explained and its possible utility discussed.

2. The minimalist model

The minimalist model is the numerical model whose largest earthquakes we will try to forecast. It was introduced in a previous work (Vázquez-Prada et al., 2002), and has mainly two, apparently contradictory, advantages for the purpose of this paper: it is simple but, at the same time, it is difficult to forecast. Because it is simple, several of its properties can be derived analytically, and it can be characterized in detail with numerical simulations which do not require an impractical amount of computer time. Because it is stochastic, it is difficult to forecast, so the results we will obtain here are not trivial. In the following paragraphs we will explain how the model works, and what are its main properties, comparing them with those of actual faults.

2.1. How the model works

The model is a simple (hence its name) cellular automaton. Cellular automata are frequently used to model seismic faults. In these models, the fault plane is divided into a grid of cells (each cell representing a fraction of the fault area), and the time evolves in discrete time steps. Each cell's state is updated at each time step according to rules that usually depend on the state of the cell or that of its neighbors in the previous time step. These rules can be designed according to certain friction laws (Ben-Zion, 2001), stress transfer (Olami et al., 1992; Hainzl et al., 1999; Preston et al., 2000), and the mechanical effects of fluids (Miller et al., 1999). In the minimalist model, as well as in other very simple cellular automata (e.g. Newman and Turcotte, 2002; González et al., 2005), these details are ignored: the model is driven stochastically, there are only two

possible states for each cell, and the earthquakes are generated according to simplified breaking rules.

Let us now explain the simplified view of earthquake generation that the model tries to sketch. In actual faults, the regional stress strains the rock blocks of the fault, making portions (patches) of the fault plane to become metastable. That is, they are static, but store enough elastic energy to propagate an earthquake rupture once triggered. Different processes (for example, fault creep —aseismic slip— and plastic deformation) dissipate stress along the fault plane, so stress is not directly converted into elastic strain. Earthquakes rupture some of the metastable patches of the fault, that then become stable, thus relieving strain. The hypocentre of an earthquake is usually located in a particularly strong patch of the fault plane, called "asperity" (Kanamori and Stewart, 1978; Aki, 1984; Das, 2003; Lei et al., 2003). Asperities appear to be persistent features where earthquake ruptures start once and again (Aki, 1984; Okada et al., 2003). Once the rupture starts, it propagates along the fault plane until it arrives at a patch of the fault that is not sufficiently strained. Then the rupture cannot propagate further, and is arrested. The relatively stable patch that is not sufficiently strained and that arrests the rupture is called the "barrier" (Das and Aki, 1977; Aki, 1984; Das, 2003).

The model, depicted in Fig. 1, sketches these features as follows. It divides the plane of a fault into an array of N equal cells, each denoted by an index i. In previous papers (Vázquez-Prada et al., 2002, 2003; López-Ruiz et al., 2004; Gómez and Pacheco, 2004; González et al., 2004), this array was drawn vertically, in order to simplify its description. Here the model will be drawn horizontally, in order to sketch the fault plane in a way more similar to that of actual faults (which are usually longer along the strike than along the dip). Some other cellular automaton models discretize the fault plane in a similar way (e.g. Rundle et al., 2004, 2006). The parameter N is the only one that can be changed in the model. The cells can only be in one of two states: "empty" (stable) or "occupied" (metastable). The state of the model at each time step can be described simply by stating which cells are occupied and which are not. The increase of regional stress, as in other simple models (Bak and Tang, 1989; Castellaro and Mulargia, 2001; Newman and Turcotte, 2002; González et al., 2005), is represented by the random addition of "stress particles". This randomness is a way of dealing with the complex stress increase in actual faults. At each time step, one cell is selected randomly, and a new particle arrives on it. That is, each cell has the same probability, $1/N$, of receiving the new stress particle. If the chosen cell is empty, the particle "occupies" it. This means that the regional stress has produced enough strain on that cell to make it metastable. If the cell is already occupied, that stress particle is lost; this is analogous to stress dissipation on the fault plane. The total number of occupied cells represents the total elastic strain on the fault.

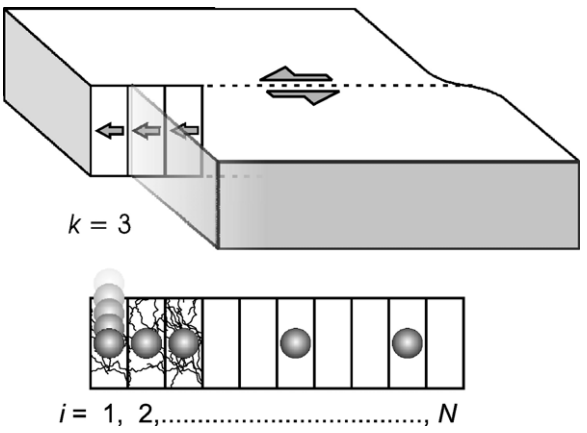

Fig. 1. The minimalist model as a sketch of a seismic fault. The fault plane is divided into an array of N equal cells, denoted with an index i, $1 \le i \le N$. The increase of regional stress is represented by the random addition of "stress particles" to the cells. Earthquake ruptures start at an asperity, the cell $i=1$, when a stress particle arrives to it. The rupture propagates through all the consecutive metastable cells (occupied by particles). The rupture area is k, the number of cells broken. The figure depicts an earthquake with $k=3$.

In the model, we assume that there is only one, persistent, asperity: the first cell, $i=1$, placed at one end of the array. This option is chosen because it simplifies the analytical description of the model. When a stress particle fills cell $i=1$, a rupture starts there, and propagates through all the consecutive metastable cells until it is arrested by a stable cell. That is, if all the successive cells $i=1$ to $i=k$ are occupied, and cell $k+1$ is empty, then the effect of the earthquake is to empty all the cells from $i=1$ to $i=k$. The other cells, $i>k$ remain unaltered. The cell $k+1$ is a barrier: it is empty (stable), so the rupture cannot propagate through it. The size (rupture area) of the earthquake is k, the number of cells broken in the synthetic earthquake. Thus, the earthquake size in the model is discrete, $1 \le k \le N$. Earthquakes, in practice, are instantaneous in the model (they do not last for any time step). This represents the fact that earthquake ruptures are, indeed, much faster than the slow stress loading represented by the addition of particles.

The random addition of particles is what makes the model stochastic. It also determines the rate at which earthquakes occur in the model. At each time step,

independently of the previous earthquake history, there is a probability $1/N$ for the incoming stress particle to arrive at cell $i=1$ and start an earthquake. Thus an earthquake, on average, occurs every N steps. The time between any two consecutive earthquakes is purely random (exponentially distributed, with rate $1/N$).

The cellular-automaton approach of this model is similar to that of the "forest fire" models, in which clusters of interconnected occupied cells ("trees") "burn" and are reset to empty when they are randomly struck by "lightning" (Drossel and Schwabl, 1992; Henley, 1993). The utility of this kind of models for earthquake physics has been noted by Rundle et al. (2003). In the minimalist model there is no random "lightning": the clusters of interconnected metastable sites are only emptied if they are connected to the cell $i=1$ *and* if this fails.

2.2. Main properties of the model

The minimalist model, because of its extreme simplicity, lacks the detailed description of the seismic process that a fully dynamical model can display. For example, it does not include the effects of fault friction, elastic stress transfer, or the role of fluids that more complex models can take into account. However, it spontaneously displays several properties that are comparable to those of actual faults, outlined as follows:

(1) *Earthquake size–frequency distribution*. It is of the characteristic earthquake type (Wesnousky et al., 1983; Schwartz and Coppersmith, 1984; Youngs and Coppersmith, 1985; Wesnousky, 1994), observed in seismic faults with simple traces (Stirling et al., 1996) and in other numerical models if the fault plane is homogeneous (e.g. Rundle and Klein, 1993; Main, 1996; Dahmen et al., 1998; Steacy and McCloskey, 1999; Moreno et al., 1999; Hainzl and Zöller, 2001; Heimpel, 2003; Zöller et al., 2005). In this distribution there is a relative excess of events (called characteristic earthquakes) which break the whole fault or most of it. In the model, they are the earthquakes with size N, and will be the events to forecast. The Gutenberg–Richter distribution (Ishimoto and Iida, 1939; Gutenberg and Richter, 1944, 1954) observed in regional seismicity (which includes contributions from many faults) can be reproduced adding up the seismicity of an ensemble of minimalist models whose sizes (N) are distributed as in actual faults (López-Ruiz et al., 2004).

(2) *Duration of the earthquake cycle*. The earthquake cycle of a fault is the time interval between two consecutive characteristic earthquakes (e.g. Scholz and Gupta, 2000). The statistical distribution of these intervals in the model is similar to the observed in seismic faults (Gómez and Pacheco, 2004). The distribution of time intervals between consecutive earthquakes of any size in the model is exponentially distributed. However, if only the characteristic earthquakes are considered, the distribution is not exponential. This is because the maximum possible size of an event depends on the size of the previous event and the time elapsed since it occurred. This is commented in the next paragraph.

(3) *Stress shadow*. When a fault generates a large earthquake, the elastic strain is reduced, and a minimum time has to elapse until the fault, by slow tectonic deformation, accumulates enough strain to generate another large earthquake. This effect is called stress shadow (Harris, 2000). In the minimalist model there is a stress shadow: if an event of size k takes place, at least k time steps have to elapse until another event of that size can occur.

(4) *Pattern of strain loading*. In actual faults, the strain increases rapidly just after a large earthquake, and then more slowly (Michael, 2005). In the model, the total elastic strain is represented by the occupation (the total number of occupied cells, Fig. 2), which has a similar pattern. Just after a large earthquake, there are fewer occupied cells, so it is more probable for the incoming particles to land on empty cells, and the occupation grows faster than later on (Fig. 2).

(5) *Seismic quiescence*. The model displays seismic quiescence (absence of earthquakes) before the

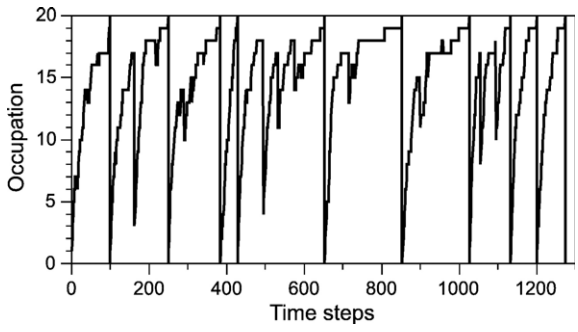

Fig. 2. The number of occupied cells in a minimalist model with $N=20$, for ten seismic cycles. This number is analogous to the total elastic strain accumulated in the fault. Sudden drops correspond to earthquakes. Each seismic cycle ends with an earthquake of size N.

characteristic events. Once $N-1$ cells (from $i=2$ to $i=N$) become occupied, the occupation reaches a plateau (Fig. 2) and, on average, N time steps have to elapse until the next earthquake (which is the characteristic one) occurs. Seismic quiescence has been observed preceding many large earthquakes (e.g. Wyss and Habermann, 1988; Scholz, 2002), although in other cases the opposite effect (increased activity) has been observed (e.g. Bowman et al., 1998; Reasenberg, 1999; Tiampo et al., 2002). The minimalist model does not show this last behaviour.

3. General scheme of forecasting

In this section we will explain the general framework for the forecasting of the largest earthquakes in the model. As a first remark, we have to consider that the model is stochastic, so it is not predictable with absolute precision. Only simple deterministic systems are fully predictable. The evolution of complex systems, such as the atmosphere or the lithosphere (even if it were deterministic) is very sensitive to the initial conditions. As these complex systems cannot be fully characterized, they turn out not to be fully predictable either.

Earthquake prediction (e.g. Keilis-Borok, 2002; Keilis-Borok and Soloviev, 2003; Rundle et al., 2003), as well as some atmospheric predictions (Mason, 2003), is frequently regarded as a binary forecast: one has to decide whether a large earthquake is going to occur or not, in a certain time-space window, instead of calculating the exact probability of this event. In this binary-forecasting approach, an "alarm" is declared when a large earthquake is expected. If it takes place when the alarm is on, the outcome is a successful forecast. If it takes place when the alarm is off, there has been a prediction failure. If the alarm was declared during a certain period, but the expected earthquake did not happen, that constitutes a false alarm.

Note that for using this approach it is necessary to define precisely what the target earthquakes are that we wish to forecast. Usually they are defined as those with a magnitude larger than a given threshold, both when dealing with actual earthquakes (e.g. Keilis-Borok and Soloviev, 2003; Rundle et al., 2003) or with synthetic ones (e.g. Pepke and Carlson, 1994; Hainzl et al., 2000). In the minimalist model, it is natural to choose as target events the characteristic earthquakes (size $k=N$), as they mark a distinct peak in the size–frequency diagram, being much more frequent than other large earthquakes (Vázquez-Prada et al., 2002, 2003).

A way to quantify the forecasting ability of a certain strategy is to compute the fraction of errors, f_e, and the fraction of alarm time, f_a (Molchan, 1997). Given a certain time series of the model, f_e is the ratio of the total number of prediction failures to the total number of target events. And f_a is the ratio of the total time during which the alarm was on to the total duration of the time series. The fraction of false alarms, f_f, is included in f_a, and is the ratio of the total duration of false alarms to the total duration of the time series.

Of course, a good forecasting strategy should render small f_a, f_e and f_f. However, as a general rule, a strategy that renders low f_e tends to produce large f_a and f_f. Dealing with real seismicity, both a failure and an alarm are costly. Eventually, decision-makers would need to consider what is less costly: to predict most of the dangerous earthquakes, but declaring many alarms, or to declare fewer alarms but failing the forecast of more large shocks (Molchan, 1997). Depending on the trade-off between costs and benefits, one should try to minimize a loss function, L, that can depend on f_a, f_e and/or f_f.

In the next section, we will describe the forecasting strategies that will be used to compare the merits of the new strategy proposed in this paper, based on synchronizing models between themselves. In the first of the subsections we will indicate the loss function we will try to minimize in the forecasting of the model.

4. Forecasting strategies for comparison

We describe here three forecasting strategies, based on the earthquake series, that we will use to asses the merits of the new strategy described later in this paper. The first two strategies (the random guessing strategy and the so called reference strategy) can be used in any system. The third is specific to the minimalist model, and serves to ideally determine its maximum theoretical predictability.

4.1. Random guessing strategy

In this strategy, the alarm is randomly turned on and off. It is simple to apply this strategy to any cellular automaton model. Here, in each time step, the alarm is on with a probability p. As a result, the alarm will be on during a fraction p of time steps ($f_a=p$). When the target earthquake finally occurs in a certain time step, there will be a probability p for the alarm to be on. Thus, on average, a fraction p of target earthquakes will be predicted, and a fraction $f_e=1-p$ will be prediction failures, so $f_a+f_e=1$. This strategy has two trivial cases:

if the alarm is always on ($f_a=1$), all the target earthquakes are "forecasted" ($f_e=0$). Conversely, if the alarm is always off ($f_a=0$), we fail to predict any of them.

To be statistically significant, any forecasting strategy must render better results than a random guess. A natural way to measure this improvement is to consider the loss function $L=f_a+f_e$. Then, $L=1$ means that the strategy performs as a random guess, and $L=0$ means a perfect prediction. If $L>1$, the strategy is performing exactly the opposite to how it should. Thus, the exact reverse strategy should be considered, and this will provide the opposite results ($f'_a=1-f_a$, and $f'_e=1-f_e$).

4.2. Reference strategy

Of course, the random guessing strategy depicted above is only useful as a baseline, but does not serve to provide a real significant forecast. In this subsection we describe the simplest meaningful forecasting strategy one can consider for any system. This will be called the reference strategy, and any forecasting procedure more complex than this should render better results.

The reference strategy consists simply in declaring an alarm some time after each target event, and maintaining it on until the next target event (e.g. Newman and Turcotte, 2002; Vázquez-Prada et al., 2003; González et al., 2005). As a general rule, the shorter this time, the bigger f_a and the lesser f_e. Which time is best, then? For the minimalist model, we can look for the number of time steps n to use with this strategy for obtaining a smaller L. In a previous paper (Vázquez-Prada et al., 2003) we observed that effectively, for each N, there is a n that minimizes L. In Fig. 3, the minimum L that can be obtained with this strategy is plotted for N between 2 and 20, as the curve labeled "Reference". This method does not generate any false alarm, nor take into account the occurrence of earthquakes smaller than the characteristic ones. The only information required is the statistical distribution (probability distribution function) of the duration of the cycles (Vázquez-Prada et al., 2003). Taking into account the effects of smaller earthquakes, the forecast can be modestly improved in the model (Vázquez-Prada et al., 2003; González et al., 2004).

4.3. Ideal strategy

As the minimalist model is very simple, it is possible to explore its maximum predictability. The ideal strategy needed for getting this result, unlike the two previously described, is model-specific. It is deduced in the Appendix. This ideal result could only be obtained if we could "see" inside the model to check at each time step which cells are occupied and which are not. Thus, it requires a perfect knowledge of the system, and equivalent strategies cannot be used with actual faults where we cannot know the detailed state of stress and strain. In the Appendix it is deduced that the alarm should be declared at the instant in which $N-1$ cells of the model are full (just at the beginning of the plateau with seismic quiescence commented on in Section 2.2). Then, it should be maintained on until the next characteristic earthquake. This is a no-error strategy ($f_e=0$, and $L=f_a$). As the model is stochastic, $_a$ is not zero; a minimum alarm time is needed to forecast all the characteristic earthquakes. It is given by $f_a=L=N/\langle n\rangle$, where $\langle n\rangle$ is the average duration of the cycles (which depends on N). This L is also plotted in Fig. 3, as the curve labelled "Ideal". This is the rigorous minimum L that can be obtained in the model. A good forecasting strategy should produce an L lower than the "Reference" curve and as close as possible to the "Ideal" curve.

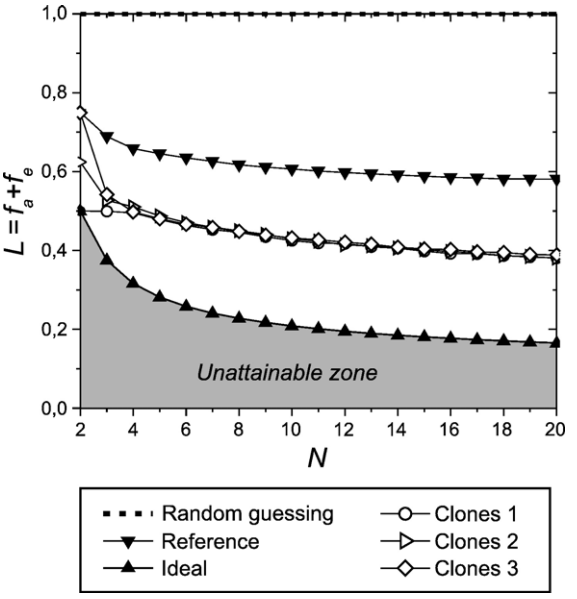

Fig. 3. Loss function (L) obtained with the different forecasting methods used in this paper, for various system sizes ($2\le N\le 20$). A random guessing strategy would render $L=1$ for any N, while $L=0$ would mean a perfect prediction. The shadowed zone is unattainable for any forecasting strategy used in the minimalist model, and the strategy that marks its upper limit is called "Ideal". The "Reference" strategy is based only on the series of the largest earthquakes in the model. The three strategies labelled "Clones" are based on the synchronization of models with the minimalist model whose largest earthquakes we try to forecast.

5. Synchronization-based forecasting

In this section we will describe the novel forecasting method based on the synchronization between models, obtained by imposing the rupture area of a minimalist model onto other similar models. This section expands and complements our previous results (González et al., 2004).

We will try to forecast the characteristic earthquakes generated by a minimalist model with N cells. This model will be called *master*. We will consider this *master* as if it were an actual fault, from which we can know the rupture area of its earthquakes (equivalent to the number of cells broken, k), but not the strain or stress at depth (equivalent to the occupation state of the model cells). As in an actual fault, we cannot change the state of the master at any moment.

In this forecasting method we will use other models, which we call *clones* (González et al., 2004). These are equivalent to the models that a scientist devises for forecasting the future evolution of the fault. We will modify their evolution at will, and their governing rules will be different than those of the master. In this paper, for simplicity, we will consider that the clones are also arrays of N cells. The average duration of the earthquake cycle in the model (average recurrence interval of the characteristic earthquakes), $\langle n \rangle$, strongly depends on N (Gómez and Pacheco, 2004). Choosing a different N for the clones will imply a different loading rate of the cells and a different average recurrence interval of the characteristic earthquakes in the clones than in the master. These effects would require further tuning of the clones, which would complicate the following discussion.

Let us describe in the following paragraphs the general outline of the procedure. We will use a total of Q clones, that will be loaded (one particle per time step and per clone) at the same time as the master, but randomly and independently to the master and to each other. We will apply some procedures for partially synchronizing the clones with the master. Namely, if in a given time step the master does not generate any earthquake, we will oblige the clones not to generate any earthquake either. And if the master does generate an earthquake, we will force the clones to reproduce the rupture area of this earthquake, as described below in more detail. Note that, although the master and the clones are driven simultaneously, the effects of the master are dealt with first.

Why use several clones? The master and the clones are all stochastic, so each one evolves with time in a different way. By using several clones, we can take into account a broad range of possible evolutions. By using only one clone, we could not be very sure that it is satisfactorily mimicking the evolution of the master. However, if several of these Q clones are in the same state, then it is more probable that the master is also in that state. If the clones were deterministic, only one would be required.

We have commented before (Section 4.3 and Appendix) that the ideal forecasting strategy for the minimalist model will be to declare the alarm just when $N-1$ cells of the model become occupied. Then the master enters the stage of seismic quiescence, or plateau, and the next earthquake is the characteristic one.We will try to determine this ideal instant as well as possible with the clones. For this, we will use a "democratic" procedure: we will declare an alarm when a minimum of q clones "vote" (become occupied to a certain threshold, described below). Later on we will explore the combinations of Q and q that render the best results. Once the alarm is declared, it is maintained on until the next earthquake in the master. If it is a characteristic one, this is a successful prediction. Its rupture is imposed on the clones (so we reset all the cells of the clones to empty) and a new cycle starts. If the next earthquake is not a characteristic one, this represents a false alarm. We will disconnect the alarm, and impose the rupture on the clones as is done with any other earthquake. Of course, if a characteristic earthquake takes place when the clones have still not declared the alarm (when less than q clones have voted), this is a prediction failure. If the clones declare an alarm in the same time step in which the master generates a characteristic earthquake, we also consider this as a prediction failure.

The exact rules for driving the clones will follow one of the three approaches commented on below. Each approach imply a different knowledge of how the master works, and a different way of imposing the rupture area on the clones. They are depicted in Fig. 4 and described as follows:

(1) This first approach will indicate which is the best result that can be obtained with the synchronization-based forecasting. For this reason, the clones are indeed minimalist models identical to the master (González et al., 2004). The clones are loaded only if the master does not generate an earthquake in that time step. We know that in this case the particle in the master has gone to one of the cells $i \geq 2$, so the particles in the clones will be randomly thrown to the cells $i \geq 2$. We also consider as known that, just after an earthquake

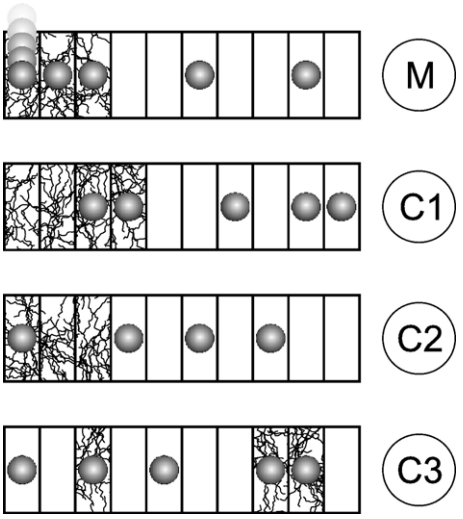

Fig. 4. Sketch that shows how the rupture area of an earthquake in the master model (M) is imposed on the clones (C), for each of the three synchronization-based approaches. In this example, the master generates an earthquake with rupture area $k=3$. In the first approach (C1), the first $k+1$ cells rupture and will be reset to empty. In the second one (C2), this occurs only with the first k cells. In the third approach (C3), this happens to k occupied cells chosen randomly. The first cell of the clones can be occupied only in the second and third approaches.

with rupture area k, the first $k+1$ cells in the master, for sure, are stable (the k just broken plus the one that acts as a barrier for the rupture). Thus, if the master generates an earthquake of size k, we will reset to empty the first $k+1$ cells of the clones. A clone votes when $N-1$ of its cells are full.

(2) In this second approach, we are more ignorant about how the master works. At every time step we will throw the stress particles to any of the cells in the clones. If the master generates an earthquake of size k, we only know which cells have ruptured, so we will reset to empty only the first k cells of the clones. A clone votes when its N cells are full.

(3) In the third approach we know even less. At every step we will throw the stress particles to any of the cells in the clones. When an earthquake takes place in the master, we only know its size, and thus its rupture area, k, but not exactly which cells have ruptured. Thus, we will randomly empty k occupied cells of each clone. If the clone has less than k occupied cells, all are emptied. A clone votes when its N cells are full. In this approach the positions of the cells in the clone are irrelevant. Each clone is thus equivalent to the so-called box model (González et al., 2005).

Note that, ideally, the clones should have the same number of occupied cells as the master. For this reason, as a way to measure the degree of synchronization between a clone and the master, we used the fraction of time, τ, during which both of them have the same number of occupied cells (González et al., 2004). If two independent masters run simultaneously, they have the same number of occupied cells, just by chance, during a certain τ. When a clone and a master are compared, this τ greatly increases, as shown in Fig. 5: partial synchronization is achieved. The best results, as expected, are achieved with the first of the three approaches.

The results of f_a, f_e, f_f and $L=f_a+f_e$, for different values of Q and q can be plotted as in the diagrams of Fig. 6. In this figure we have plotted only results corresponding to the first of the three approaches and $N=20$, but similar figures, with the same overall

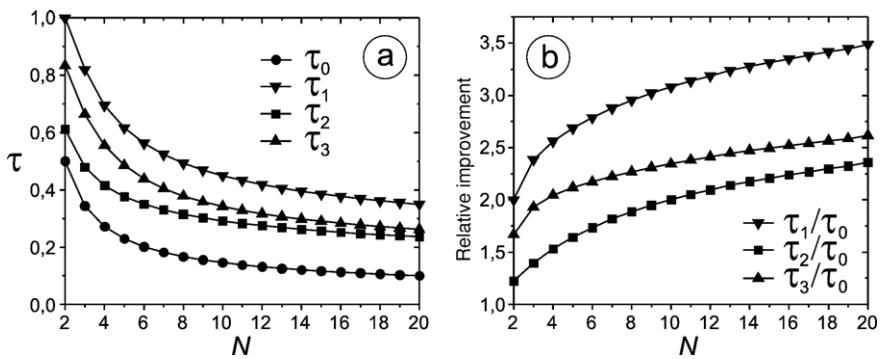

Fig. 5. (a) The fraction of time, τ, during which two models have the same number of occupied cells. This depends on whether they are two independent masters (τ_0) or a master and a clone (governed by one of the three different synchronization approaches: τ_1, τ_2 and τ_3). (b) The relative improvement, defined as τ_n/τ_0.

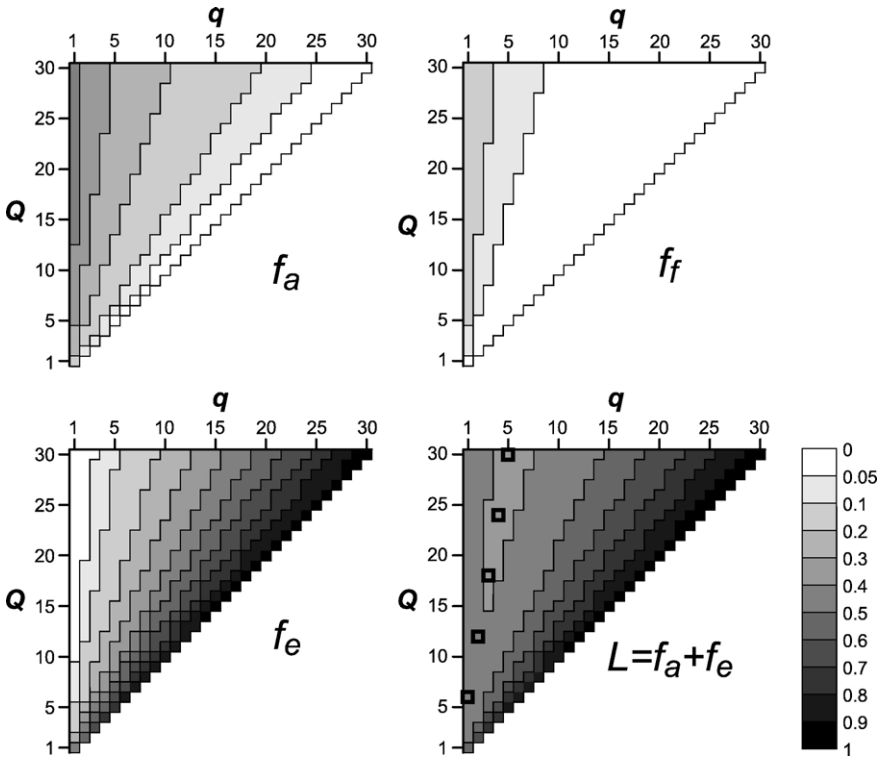

Fig. 6. Fraction of alarm time (f_a), fraction of false alarm time (f_f), fraction of errors (f_e), and loss function (L) obtained with the the first synchronization-based forecasting approach, for $N=20$ and different numbers of clones (Q) and votes (q). The squared cells mark a rectilinear valley in the values of L.

properties, can be drawn for the other two approaches and for any N (see below). There are simple trends in these graphs. In Section 3 we noted that, in general, a forecasting strategy that produces lower f_e tends to produce higher f_a and f_f. If Q is fixed (same row), the greater the q, the later the alarm is declared, so f_a and f_f are lesser and f_e is greater. If q is fixed (same column), the greater the Q, the earlier the alarm is declared, resulting in the opposite trend.

We are interested in finding the combinations of Q and q that minimize L. The interesting fact is that the sum f_a+f_e shows a rectilinear "valley" for certain combinations of Q and q, marked with squares in the graph of Fig. 6. This valley goes down as Q and q increase. In Fig. 7 it can be observed that the valley goes down indefinitely, tending to a lowest asymptotic value of L. We estimate this value, as a function of Q, with a three-parameter exponential fit of the form $F=a\exp[b/(Q+c)]$, where a, b, and c are parameters (Fig. 7). The value of a is the asymptotic one for $Q\to\infty$. This value is represented, for each N, in Fig. 3. The f_a, f_f and f_e also have asymptotic trends along this valley of L, also plotted in Fig. 7. They can also be fitted with the same kind of three-parameter distribution, to estimate their asymptotic values as $Q\to\infty$. A nice property is that, as shown in Fig. 7 for a certain case, these forecasting approaches predict most of the characteristic earthquakes (f_e is low), and have a

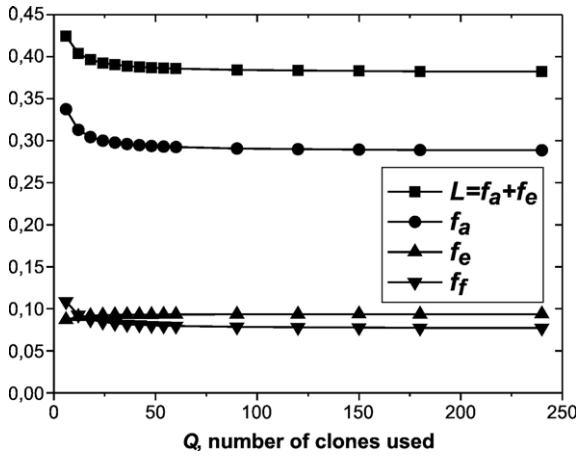

Fig. 7. Loss function (L), fraction of alarm time (f_a), fraction of false alarm time (f_f) and fraction of errors (f_e) obtained with the first synchronization-based forecasting approach, for $N=20$ and different numbers of clones (Q) along the rectilinear valley observed in L in Fig. 6 (the first five points of each curve correspond to the cells marked in that figure). The curves are exponential fits with three parameters.

very small fraction of false alarms. Note also that a few tens of clones already render results close to the asymptotic ones.

As can be noted in Fig. 3, the synchronization-based strategies perform much better than a random guess, and also much better than the reference strategy described in Section 4.2. Their results are intermediate between the ideal forecast and the reference one. The second and third synchronization-based approaches give only slightly greater L than the first one. The differences are large only for small N. Although the first approach synchronizes more efficiently each individual clone with the master (Fig. 5), this effect is compensated by using many clones.

To assess the performance of the method with larger systems, we plot in Fig. 8 the results of L for the three approaches, for $N=100$ and up to 60 clones. As occurred for smaller N, a rectilinear valley is observed in the graphs, and this tendency can be extrapolated to estimate the asymptotic value of L. Note that the results for the first and second approaches are almost identical (although L is slightly larger in the second approach). With the third approach, L decays to its asymptotic value more slowly (the valley floor has a smaller slope, so more clones are needed to achieve a given low L). The asymptotic values of L, however, are very similar in the three cases (0.298 for the first and second approaches; 0.306 for the third one). Note that these values are smaller than for $N=20$, as expected from the trend observed in Fig. 3. The f_a, f_e and f_f show trends similar to the ones described for Figs. 6 and 7. The asymptotic f_e is very low (0.062, 0.075 and 0.071 for the first, second, and third approach, respectively).

Another way to measure the synchronization of the clones with the master is drawn in Fig. 9 for $N=20$. The ideal strategy (Section 4.3 and Appendix), would be to declare the alarm just when $N-1$ cells of the master are full. The figure shows how a single clone declares the alarm around that moment, but a group of clones does a much better job.

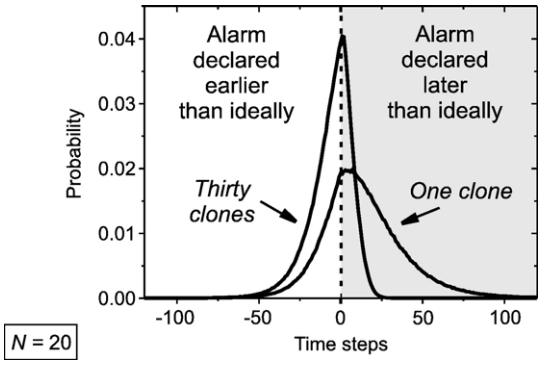

Fig. 9. Probability that a clone or thirty clones (with $q=5$; the uppermost squared cell in L in Fig. 6) declare an alarm in a given time, around the instant when it should for obtaining the ideal forecast.

6. Discussion and conclusions

In this paper we have tried to provide some insight into how to synchronize numerical models with seismic faults, in order to better forecast large earthquakes in them. The idea is that, although we can rarely measure the stress and strain in actual faults, we can estimate the rupture area and co-seismic displacement of their earthquakes. If we force a calibrated model to reproduce every earthquake rupture of the fault it simulates, probably the model will be synchronized with the fault. Then it could be used to forecast the future evolution of the fault, including future large earthquakes. This idea is not completely new: e.g. Ward (2000) forced a model to reproduce a large-earthquake rupture and run the model forward to see what could happen in the future. The results of this paper expand on earlier ones (González et al., 2004), and are still only theoretical, but fully

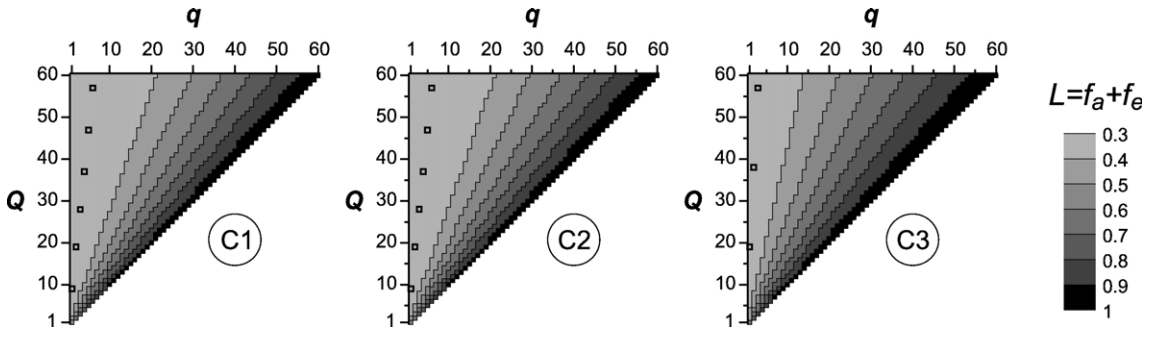

Fig. 8. Loss function (L) obtained with the three synchronization-based forecasting approaches, for $N=100$ and different numbers of clones (Q) and votes (q). The squared cells mark rectilinear valleys in the values of L.

quantitative. We demonstrate that it is possible to partially synchronize numerical fault models between themselves, and use this to forecast synthetic earthquakes.

One of the models, called the master, evolves freely. We consider it as an actual fault, from which we can know the rupture area of its earthquakes, but not the strain or stress at depth. Our goal is to forecast the largest earthquakes it generates. In the synchronization-based forecasting, we use several other models, called clones, similar to the master (calibrated to have the same average recurrence interval of large earthquakes that the master has). These clones are equivalent to the models that can be devised to simulate a seismic fault. They are run simultaneously and independently to the master and to each other. We force them to reproduce the series of earthquake ruptures of the master, and this makes them partially synchronized with it. In simple words, if the master does not generate an earthquake, we preclude any earthquake in the clones; if the master does generate an earthquake, we impose the same rupture area on the clones. When several of the clones are highly loaded (strained), we declare an alarm, because the master is probably also highly loaded, and thus probably a large earthquake is impending. This procedure efficiently predicts most of the largest earthquakes of the master, with a relatively low fraction of total alarm time and few false alarms. These results are robust: they are almost the same when the exact rules for imposing the earthquake ruptures vary, and this good performance is observed along the whole range of model sizes considered. This synchronization-based forecasting outperforms other procedures based only on the earthquake series of the model (Vázquez-Prada et al., 2003; González et al., 2004).

The master and the clones are stochastic (random), so each individual clone is only partially synchronized with the master. However, when several clones are in the same state, then it is more likely that the master is also in this state, so the group of clones makes a much better forecasting job than only one clone does. If the clones were deterministic, as a general rule only one would be needed; more clones would have identical evolutions if run with the same initial conditions.

The procedure developed here is a kind of ensemble forecasting, in which several models are run to obtain a better picture of how a system will evolve. This concept is used in atmospheric forecasting (Palmer et al., 2005): several models are run simultaneously, and their average result has a larger forecasting ability than that of an individual model (Houghton, 2002; Palmer et al., 2005). Each model in this approach has slightly different initial conditions, to take into account measurement errors and then to represent one possible state of the atmosphere, among various possibilities. In our approach, each clone marks a possible state of the master among a range of possible options. Several deterministic clones could also be used with different initial conditions.

Our procedure also shares some similarities with certain earthquake forecasting algorithms (Kossobokov et al., 1999; Keilis-Borok and Soloviev, 2003), in which several seismicity functions are evaluated in real-time. When several of these functions indicate that a large earthquake is probable, an alarm is declared. In our approach, the clones are performing a role similar to these functions, monitoring what is happening in the master.

Our proposal is that a possible way to synchronize more complex, calibrated models with real faults might be to force them to reproduce the past series of earthquakes (with the same rupture area and/or co-seismic displacement). This would need to be tested in the future. Also it will be possible to test whether this procedure works in the forecasting of synthetic earthquakes in other models.

Forcing the models to reproduce only one large observed rupture (as in Ward, 2000) probably is not enough (this is certainly the case in our stochastic model). Complex and chaotic systems, such as the lithosphere, are very sensitive to initial conditions. Forcing the model to reproduce only one rupture is a necessary and laudable first step, but probably does not constrain the initial conditions sufficiently. We propose that every observed rupture, albeit small, should be considered. Small earthquakes are much more frequent than large ones, thus providing much more data. Moreover, they provide insight into the mechanical state of the crust (Seeber and Armbruster, 2000) and into the mechanics of earthquake rupture (Rubin, 2002). They may indicate the patch of the fault plane which is experiencing higher stresses and is likely to rupture in the next large shock (Schorlemmer and Wiemer, 2005). Finally, they are important in the transfer of stress within the lithosphere, and in earthquake triggering (Helmstetter et al., 2005).

Acknowledgments

Á.G. thanks Robert Shcherbakov for helping him to view the model with new eyes. We benefited from the reviews by Kristy F. Tiampo and an anonymous reviewer. Part of the numerical simulations were done in the computer cluster of the Institute of Biocomputing and Physics of Complex Systems (BIFI), at the University of Zaragoza. The Spanish Ministry of

Education and Science funded this research by means of the project FIS2005-06237, and the grant AP2002-1347 held by Á.G.

Appendix A. Deduction of the ideal forecasting strategy

In this appendix we will deduce the ideal strategy outlined in Section 4.3. This strategy renders the lowest (best) value of $L=f_a+f_e$ achievable in the minimalist model.

For this reasoning we would consider every cycle of the model as composed of two independent and consecutive stages. The first, that will be called the *loading* stage, starts just after the occurrence of a characteristic earthquake. During this stage the total number of occupied cells grows, but not in a monotonic way, because the particles may land in already occupied cells (and then be dissipated), and also because of the occurrence of non-characteristic earthquakes (Fig. 2). When $N-1$ cells (all but the first one) become occupied, this first stage ends and the second stage, that will be called the *hitting* stage (or plateau in the occupation), starts. In this second stage, the system resides statically in the state of maximum occupancy (Fig. 2) until a particle arrives at the first cell. Then, a characteristic event occurs, all the cells are emptied, and a new cycle begins. The hitting stage can be mathematically treated as a form of Russian roulette.

Both the time spent by the system in the loading stage, x, and in the hitting stage, y, are statistically distributed. The distribution of y, denoted by $P_2(y)$, is geometric. Considering that, in each time step, the probability of hitting the first cell is $p=1/\mathrm{N}$, and its complementary is $q=1-1/N$, it follows that

$$P_2(y)=\frac{1}{N}\left(1-\frac{1}{N}\right)^{y-1}, \tag{A.1}$$

whose mean is

$$\langle y\rangle = N, \tag{A.2}$$

and whose standard deviation is

$$\sigma = N\sqrt{1-\frac{1}{N}}. \tag{A.3}$$

The time elapsed between consecutive characteristic events has been denoted by n, which is statistically distributed according to the function $P_N(n)$ (Vázquez-Prada et al., 2002, 2003; Gómez and Pacheco, 2004). Because the variables x and y are independent, the mean length of the cycles $\langle n\rangle$ is the sum of the mean lengths of the two stages:

$$\langle n\rangle = \langle x\rangle + \langle y\rangle. \tag{A.4}$$

It is clear that the best L would be obtained only if we knew the state of occupation of the system and could mark, for each cycle, the instant at which the stage of loading concludes. Let us explore the result of L obtained if we turn the alarm on at a given value $y=y_0$ within the second stage of all the cycles. With this strategy, the fraction of errors is given by

$$f_e(y_0)=\sum_1^{y_0} P_2(y) \tag{A.5}$$

and inserting Eq. (A.1) we obtain

$$f_e(y_0)=1-q^{y_0}. \tag{A.6}$$

With respect to the fraction of alarm, its form is

$$f_a(y_0)=\frac{\sum_{y=y_0}^{\infty}(y-y_0)\cdot P_2(y)}{\langle x\rangle+\langle y\rangle}, \tag{A.7}$$

and inserting Eq. (A.1), we get

$$f_a(y_0)=\frac{Nq^{y_0}}{\langle x\rangle+N}. \tag{A.8}$$

Note the important contribution of the first stage of the process in the denominator. Thus, the specific form of the loss function is

$$L(y_0)=1-q^{y_0}+\frac{Nq^{y_0}}{\langle x\rangle+N}. \tag{A.9}$$

It is noteworthy that in the absence of the first stage, i.e. in the hypothesis of a pure geometric distribution, the value of L would be 1, not dependent on the value of y_0. The minimum value of L in Eq. (A.9) as a function of y_0 is obtained for $y_0=0$, i.e. just after the end of the first stage, when the $N-1$ upper cells of the system become full. And this minimum value is

$$L_{\min}=\frac{N}{\langle n\rangle}. \tag{A.10}$$

This result constitutes a rigorous lower bound for the expected accuracy of any forecasting strategy in the minimalist model. For this model, $\langle n\rangle$ increases rapidly as N grows (Gómez and Pacheco, 2004). This implies that the minimum L, obtained with this optimal forecasting strategy, decreases as N increases, as shown by the curve labeled as "Ideal" in Fig. 3. That is to say, minimalist models with more cells are more

predictable. This is consistent with the fact that the time series of characteristic earthquakes is more periodic for larger N (Gómez and Pacheco, 2004).

References

Aki, K., 1984. Asperities, barriers, characteristic earthquakes and strong motion prediction. Journal of Geophysical Research 89, 5867–5872.

Baba, T., Cummins, P.R., 2005. Contiguous rupture areas of two Nankai Trough earthquakes revealed by high-resolution tsunami waveform inversion. Geophysical Research Letters 32, L08305.

Bak, P., Tang, C., 1989. Earthquakes as a self-organized critical phenomenon. Journal of Geophysical Research 94, 15635–15637.

Ben-Zion, Y., 2001. Dynamic ruptures in recent models of earthquake faults. Journal of the Mechanics and Physics of Solids 49, 2209–2244.

Boness, N.L., Zoback, M.D., 2004. Stress-induced seismic velocity anisotropy and physical properties in the SAFOD Pilot Hole in Parkfield, CA. Geophysical Research Letters 13, L15S17.

Bowman, D.D., Ouillon, G., Sammis, C.G., Sornette, A., Sornette, D., 1998. An observational test of the critical earthquake concept. Journal of Geophysical Research 103, 24359–24372.

Castellaro, S., Mulargia, F., 2001. A simple but effective cellular automaton for earthquakes. Geophysical Journal International 144, 609–624.

Dahmen, K., Ertaş, D., Ben-Zion, Y., 1998. Gutenberg–Richter and characteristic earthquake behavior in simple mean-field models of heterogeneous faults. Physical Review E 58, 1494–1501.

Das, S., 2003. Spontaneous complex earthquake rupture propagation. Pure and Applied Geophysics 160, 579–602.

Das, S., Aki, K., 1977. Fault plane with barriers: a versatile earthquake model. Journal of Geophysical Research 82, 5658–5670.

Dowrick, D.J., Rhoades, D.A., 2004. Relations between earthquake magnitude and fault rupture dimensions: how regionally variable are they? Bulletin of the Seismological Society of America 94, 776–788.

Drossel, B., Schwabl, F., 1992. Self-organized criticality in a forest-fire model. Physica A 191, 47–50.

Fitzenz, D.D., Miller, S.A., 2004. New insights on stress rotations from a forward regional model of the San Andreas fault system near its Big Bend in southern California. Journal of Geophysical Research 109, B08404.

Goltz, C., 1997. Fractal and Chaotic Properties of Earthquakes. Springer-Verlag, Berlin, Germany, p. 178.

Gómez, J.B., Pacheco, A.F., 2004. The minimalist model of characteristic earthquakes as a useful tool for description of the recurrence of large earthquakes. Bulletin of the Seismological Society of America 94, 1960–1967.

González, Á., Vázquez-Prada, M., Gómez, J.B., Pacheco, A.F., 2004. Using synchronization to improve the forecasting of large relaxations in a cellular-automaton model. Europhysics Letters 68, 611–617.

González, Á., Gómez, J.B., Pacheco, A.F., 2005. The occupation of a box as a toy model for the seismic cycle of a fault. American Journal of Physics 73, 946–952.

Grant, L.B., Gould, M.M., 2004. Assimilation of paleoseismic data for earthquake simulation. Pure and Applied Geophysics 161, 2295–2306.

Gutenberg, B., Richter, C.F., 1944. Frequency of earthquakes in California. Bulletin of the Seismological Society of America 34, 185–188.

Gutenberg, B., Richter, C.F., 1954. Seismicity of the Earth and Associated Phenomena, 2nd edn. Princeton University Press, Princeton, New Jersey, USA, p. 310.

Hainzl, S., Zöller, G., 2001. The role of disorder and stress concentration in nonconservative fault systems. Physica A 294, 67–84.

Hainzl, S., Zöller, G., Kurths, J., 1999. Self-organized criticality model for earthquakes: quiescence, foreshocks and aftershocks. International Journal of Bifurcation and Chaos 9, 2249–2255.

Hainzl, S., Zöller, G., Kurths, J., Zschau, J., 2000. Seismic quiescence as an indicator for large earthquakes in a system of self-organized criticality. Geophysical Researh Letters 27, 597–600.

Harris, R.A., 2000. Earthquake stress triggers, stress shadows, and seismic hazard. Current Science 79, 1215–1225.

Hashimoto, M., 2001. Complexity in the recurrence of large earthquakes in southwestern Japan: a simulation with an interacting fault system model. Earth, Planets and Space 53, 249–259.

Heimpel, M.H., 2003. Characteristic scales of earthquake rupture from numerical models. Nonlinear Processes in Geophysics 10, 573–584.

Helmstetter, A., Kagan, Y.Y., Jackson, D.D., 2005. Importance of small earthquakes for stress transfers and earthquake triggering. Journal of Geophysical, Research 110, B05S08.

Henley, C.L., 1993. Statics of a "self-organized" percolation model. Physical Review Letters 71, 2741–2744.

Hickman, S., Zoback, M., 2004. Stress orientations and magnitudes in the SAFOD pilot hole. Geophysical Research Letters 31, L15S12.

Houghton, J., 2002. The Physics of Atmospheres. Cambridge University Press, Cambridge, UK, p. 320.

Ikeda, R., Iio, Y., Omura, K., 2001. In situ stress measurements in NIED boreholes in and around the fault zone near the 1995 Hyogoken Nanbu earthquake, Japan. The Island Arc 10, 252–260.

Ishimoto, M., Iida, K., 1939. Observations sur les séismes enregistrés par le microséismographe construit dernièrement (I). Bulletin of the Earthquake Research Institute, University of Tokyo 17, 443–478.

Kanamori, H., Brodsky, E.E., 2004. The physics of earthquakes. Reports on Progress in Physics 67, 1429–1496.

Kanamori, H., Stewart, G.S., 1978. Seismological aspects of Guatemala earthquake on February 4, 1976. Journal of Geophysical Research 83, 3427–3434.

Kato, N., Seno, T., 2003. Hypocenter depths of large interplate earthquakes and their relation to seismic coupling. Earth and Planetary Science Letters 210, 53–63.

Keilis-Borok, V.I., 2002. Earthquake prediction: state-of-the-art and emerging possibilities. Annual Review of Earth and Planetary Sciences 30, 1–33.

Keilis-Borok, V.I., Soloviev, A.A. (Eds.), 2003. Nonlinear Dynamics of the Lithosphere and Earthquake Prediction. Springer, Berlin, p. 337.

Kisslinger, C., 1996. Aftershocks and fault-zone properties. Advances in Geophysics 38, 1–36.

Kossobokov, V.G., Romashkova, L.L., Keilis-Borok, V.I., Healy, J. H., 1999. Testing earthquake prediction algorithms: statistically significant advance prediction of the largest earthquakes in the Circum-Pacific, 1992–1997. Physics of the Earth and Planetary Interiors 111, 187–196.

Kuroki, H., Ito, H.M., Takayama, H., Yoshida, A., 2004. 3-D simulation of the occurrence of slow slip events in the Tokai

region with a rate- and state-dependent friction law. Bulletin of the Seismological Society of America 94, 2037–2050.
Lei, X., Kusunose, K., Satoh, T., Nishizawa, O., 2003. The hierarchical rupture process of a fault: an experimental study. Physics of the Earth and Planetary Interiors 137, 213–228.
López-Ruiz, R., Vázquez-Prada, M., Gómez, J.B., Pacheco, A.F., 2004. A model of characteristic earthquakes and its implications for regional seismicity. Terra Nova 16, 116–120.
Main, I., 1996. Statistical physics, seismogenesis, and seismic hazard. Reviews of Geophysics 34, 433–462.
Mason, I.B., 2003. Binary forecasts. In: Joliffe, I.T., Stephenson, D.B. (Eds.), Forecast Verification: A Practitioner's Guide in Atmospheric Science. Wiley, West Sussex, UK, pp. 37–76. References in pp. 215–226.
Michael, A.J., 2005. Viscoelasticity, postseismic slip, fault interactions, and the recurrence of large earthquakes. Bulletin of the Seismological Society of America 95, 1594–1603.
Miller, S.A., Ben-Zion, Y., Burg, J.-P., 1999. A three-dimensional fluid-controlled earthquake model: behavior and implications. Journal of Geophysical Research 104, 10621–10638.
Molchan, G.M., 1997. Earthquake prediction as a decision-making problem. Pure and Applied Geophysics 149, 233–247.
Moreno, Y., Gómez, J.B., Pacheco, A.F., 1999. Self organized criticality in a fiber-bundle-type model. Physica A 274, 400–409.
Newman, W.I., Turcotte, D.L., 2002. A simple model for the earthquake cycle combining self-organized complexity with critical point behavior. Nonlinear Processes in Geophysics 9, 453–461.
Okada, T., Matsuzawa, T., Hasegawa, A., 2003. Comparison of source areas of M4.8±0.1 repeating earthquakes off Kamaishi, NE Japan: are asperities persistent features? Earth and Planetary Science Letters 213, 361–374.
Olami, Z., Feder, H.J.S., Christensen, K., 1992. Self-organized criticality in a continuous, nonconservative cellular automaton modeling earthquakes. Physical Review Letters 68, 1244–1247.
Palmer, T.N., Shutts, G.J., Hagedorn, R., Doblas-Reyes, F.J., Jung, T., Leutbecher, M., 2005. Representing model uncertainty in weather and climate prediction. Annual Review of Earth and Planetary Sciences 33, 163–193.
Pepke, S.L., Carlson, J.M., 1994. Predictability of self-organizing systems. Physical Review E 50, 236–242.
Preston, E.F., Sá Martins, J.S., Rundle, J.B., Anghel, M., Klein, W., 2000. Models of earthquake faults with long-range stress transfer. Computing in Science and Engineering 2, 34–41.
Reasenberg, P.A., 1999. Foreshock occurrence rates before large earthquakes worldwide. Pure and Applied Geophysics 155, 355–379.
Reinecker, J., Heidbach, O., Tingay, M., Sperner, B., Müller, B., 2005. The release 2005 of the World Stress Map (available online at www.world-stressmap. org).
Robinson, R., 2004. Potential earthquake triggering in a complex fault network: the northern South Island, New Zealand. Geophysical Journal International 159, 734–748.
Robinson, R., Benites, R., 2001. Upgrading a synthetic seismicity model for more realistic fault ruptures. Geophysical Research Letters 28, 1843–1846.
Rubin, A.M., 2002. Aftershocks of microearthquakes as probes of the mechanics of rupture. Journal of Geophysical Research 107, 2142.
Rundle, J.B., Klein, W., 1993. Scaling and critical phenomena in a cellular automaton slider-block model for earthquakes. Journal of Statistical Physics 72, 405–413.
Rundle, P.B., Rundle, J.B., Tiampo, K.F., Sa Martins, J.S., McGinnis, S., Klein, W., 2001. Nonlinear network dynamics on earthquake fault systems. Physical Review Letters 87, 148501.
Rundle, J.B., Turcotte, D.L., Shcherbakov, R., Klein, W., Sammis, C., 2003. Statistical physics approach to understanding the multiscale dynamics of earthquake fault systems. Reviews of Geophysics 41, 1019.
Rundle, J.B., Rundle, P.B., Donnellan, A., Fox, G., 2004. Gutenberg–Richter statistics in topologically realistic system-level earthquake stress-evolution simulations. Earth, Planets and Space 56, 761–771.
Rundle, J.B., Rundle, P.B., Donnellan, A., Li, P., Klein, W., Morein, G., Turcotte, D.L., Grant, L., 2006. Stress transfer in earthquakes, hazard estimation and ensemble forecasting: inferences from numerical simulations. Tectonophysics 413, 109–125.
Scholz, C.H., 2002. The Mechanics of Earthquakes and Faulting, 2nd edn. Cambridge University Press, Cambridge, UK, p. 496.
Scholz, C.H., Gupta, A., 2000. Fault interactions and seismic hazard. Journal of Geodynamics 29, 459–467.
Schorlemmer, D., Wiemer, S., 2005. Microseismicity data forecast rupture area. Nature 434, 1086.
Schwartz, D.P., Coppersmith, K.J., 1984. Fault behavior and characteristic earthquakes: examples from the Wasatch and San Andreas fault zones. Journal of Geophysical Research 89, 5681–5698.
Seeber, L., Armbruster, J.G., 2000. Earthquakes as beacons of stress change. Nature 407, 69–72.
Sieh, K., 1996. The repetition of large-earthquake ruptures. Proceedings of the National Academy of Sciences of the United States of America 93, 3764–3771.
Soloviev, A., Ismail-Zadeh, A., 2003. Models of dynamics of block-and-fault systems. In: Keilis-Borok, V.I., Soloviev, A.A. (Eds.), Nonlinear Dynamics of the Lithosphere and Earthquake Prediction. Springer, Berlin, Germany, pp. 71–139. References in pp. 311–332.
Steacy, S.J., McCloskey, J., 1999. Heterogeneity and the earthquake magnitude–frequency distribution. Geophysical Research Letters 26, 899–902.
Stirling, M.W., Wesnousky, S.G., Shimazaki, K., 1996. Fault trace complexity, cumulative slip, and the shape of the magnitude–frequency distribution for strike–slip faults: a global survey. Geophysical Journal International 124, 833–868.
Stirling, M., Rhoades, D., Berryman, K., 2002. Comparison of earthquake scaling relations derived from data of the instrumental and preinstrumental era. Bulletin of the Seismological Society of America 92, 812–830.
Tanioka, Y., Hirata, K., Hino, R., Kanazawa, T., 2004. Slip distribution of the 2003 Tokachi-oki earthquake estimated from tsunami waveform inversion. Earth, Planets and Space 56, 373–376.
Tiampo, K.F., Rundle, J.B., McGinnis, S.A., Klein, W., 2002. Pattern dynamics and forecast methods in seismically active regions. Pure and Applied Geophysics 159, 2429–2467.
Tsukahara, H., Ikeda, R., Yamamoto, K., 2001. In situ stress measurements in a borehole close to the Nojima Fault. The Island Arc 10, 261–265.
Turcotte, D.L., 1997. Fractals and Chaos in Geology and Geophysics, 2nd edition. Cambridge University Press, Cambridge, UK, p. 412.
Vázquez-Prada, M., González, Á., Gómez, J.B., Pacheco, A.F., 2002. A minimalist model of characteristic earthquakes. Nonlinear Processes in Geophysics 9, 513–519.

Vázquez-Prada, M., González, Á., Gómez, J.B., Pacheco, A.F., 2003. Forecasting characteristic earthquakes in a minimalist model. Nonlinear Processes in Geophysics 10, 565–571.

Ward, S.N., 2000. San Francisco Bay area earthquake simulations: a step toward a standard physical earthquake model. Bulletin of the Seismological Society of America 90, 370–386.

Wells, D.L., Coppersmith, K.J., 1994. New empirical relationships among magnitude, rupture length, rupture width, rupture area, and surface displacement. Bulletin of the Seismological Society of America 84, 974–1002.

Wesnousky, S.G., 1994. The Gutenberg–Richter or characteristic earthquake distribution, which is it? Bulletin of the Seismological Society of America 84, 1940–1959.

Wesnousky, S.G., Scholz, C.H., Shimazaki, K., Matsuda, T., 1983. Earthquake frequency distribution and the mechanics of faulting. Journal of Geophysical Research 88, 9331–9340.

Wyss, M., Habermann, R.E., 1988. Precursory seismic quiescence. Pure and Applied Geophysics 126, 319–332.

Yabuki, T., Matsu'ura, M., 1992. Geodetic data inversion using a bayesian information criterion for spatial-distribution of fault slip. Geophysical Journal International 109, 363–375.

Yagi, Y., Kikuchi, M., Yoshida, S., Sagiya, T., 1999. Comparison of the coseismic rupture with the aftershock distribution in the Hyuga-nada earthquakes of 1996. Geophysical Research Letters 26, 3161–3164.

Yamamoto, K., Yabe, Y., 2001. Stresses at sites close to the Nojima Fault measured from core samples. The Island Arc 10, 266–281.

Yeats, R.S., Sieh, K., Allen, C.R., 1997. The Geology of Earthquakes. Oxford University Press, New York, USA, p. 568.

Youngs, R.R., Coppersmith, K.J., 1985. Implications of fault slip rates and earthquake recurrence models to probabilistic seismic hazard estimates. Bulletin of the Seismological Society of America 75, 939–964.

Zoback, M.L., 1992. 1st-order and 2nd-order patterns of stress in the lithosphere — The World Stress Map project. Journal of Geophysical Research 97, 11703–11728.

Zöller, G., Holschneider, M., Ben-Zion, Y., 2005. The role of heterogeneities as a tuning parameter of earthquakes dynamics. Pure and Applied Geophysics 162, 1027–1049.